

## Probing the History of Cluster Assembly by Intracluster Planetary Nebulae

Sadanori Okamura

*Department of Astronomy and Research Center for the Early Universe,  
School of Science, the University of Tokyo, Tokyo, 113-0033 Japan*

**Abstract.** We describe the results and the current status of our program to search for intracluster planetary nebulae (ICPNe) in the Virgo and the Coma clusters of galaxies. For the Virgo cluster, ICPNe candidates were detected with narrow band imaging combined with broad band imaging. The use of two narrow band filters for  $H\alpha$  and [O III] lines tuned for the cluster redshift enabled us to detect secure ICPNe candidates. Kinematics of the detected ICPNe confirm that the Virgo cluster is in a highly unrelaxed state. In order to detect ICPNe in the Coma cluster, which is more than five times more distant than the Virgo cluster, we devised a multi-slit imaging spectroscopy technique and successfully detected 35 secure ICPNe candidates for the first time in this cluster. We have found a hint that the Coma cluster is currently in the midst of a subcluster merger.

### 1. Introduction

Cosmological simulations predict that a substantial fraction of stars in galaxies were stripped off during the assembly of a cluster of galaxies. These stars were dispersed into intracluster space and now recognized as the intracluster stellar population. This population is a sensitive probe of cluster assembly, and more generally, structure formation of the universe. The total amount, spatial distribution (morphology), kinematics, and metallicity are among the key parameters which characterize the population.

The intracluster stellar population has been observed as diffuse intracluster light (Mihos et al. 2005; Krick et al. 2006), or as individual stars, i.e., planetary nebulae (Arnaboldi et al. 1996; Okamura et al. 2002), or as red giant stars (Ferguson et al. 1998). The intracluster planetary nebulae (ICPNe) are the only probe that enables us to investigate the kinematics of the intracluster stellar population. We launched a program to search for ICPNe in clusters of galaxies with a range of properties on the advent of Subaru telescope and its wide-field Camera, Suprime-Cam.

### 2. Observing Strategy

Initial targets of our program are the Virgo cluster at the distance of  $(m-M)_0 \sim 31$  and the Coma cluster at  $(m-M)_0 \sim 35$ . The Virgo cluster is irregular and loose in shape, and dynamically unrelaxed containing a considerable fraction of spiral galaxies, while the Coma cluster is regular and rich in shape, and dynamically more relaxed than the Virgo cluster.

We applied a conventional narrow band plus broad band imaging technique to the nearby Virgo cluster. Unique feature of our search is the use of two narrow band filters for  $H\alpha$  and [O III] lines tuned for the cluster redshift. Previous planetary nebula searches over the image of Virgo ellipticals (e.g, Jacoby et al. 1990, hereafter JCF) used the strongest [O III] line only. The PNe candidates selected by the [O III] single line technique is contaminated by foreground and background emission line objects. Especially, when the single line technique is used to search for ICPNe in the 'blank region' free from Virgo member galaxies, the contamination could dominate the candidates. Use of the two lines and broad band images enabled us to identify secure ICPNe candidates. However, the follow-up spectroscopy is necessary to the final confirmation and kinematic studies. We used Telescopio Nazionale Galileo (TNG) 4 m telescope and Very Large Telescope (VLT) for the follow-up spectroscopy.

No imaging technique can be successfully applied to the detection of ICPNe in the distant Coma cluster. At the Coma distance, even the brightest PN is buried in the sky noise and undetectable in the narrow band image. Increase of the signal-to-noise ratio of the emission lines by reducing the sky noise is critically important. To achieve this, we devised a multi-slit imaging spectroscopy (MSIS) technique, which was successfully applied to the Coma cluster.

### 3. Virgo Cluster

#### 3.1. Imaging Observation and Selection Criteria

Observations, selection criteria for secure PNe candidates, and initial results were described in Okamura et al. (2002) and Arnaboldi et al. (2003). Only the outline is repeated here.

In 2001 March - April a field in the Virgo Cluster at  $(\alpha, \delta)(J2000) = (12^h 25^m 47.^s 0, +12^\circ 43' 58'')$ , just south of M84-M86, was observed during the commissioning of the Suprime-Cam (Miyazaki et al. 2002), at the prime focus of the Subaru 8.2 m telescope (Iye et al. 2004). Suprime-Cam covers an area of  $34' \times 27'$  of the sky, with a resolution of  $0.''2 \text{ pixel}^{-1}$ . The field was imaged through two narrow band and two broadband ( $V$  and  $R$ ) filters. The two narrow band filters have  $(\lambda_c, \Delta\lambda) = (5021\text{\AA}, 74\text{\AA})$  and  $(6607\text{\AA}, 101\text{\AA})$ , corresponding to the [O III] and  $H\alpha$  emissions at the redshift of the Virgo cluster. Exposure times are 900, 720, 3600, and 8728 seconds for  $V$ ,  $R$ , [O III], and  $H\alpha$ , respectively.

We use the two-color diagram [O III] -  $H\alpha$  versus [O III] - ( $V+R$ ) to select our emission-line objects. Simulated populations of PNe, single-lined emitters, and continuum sources were constructed and used to outline the regions in the two-color diagram inhabited by the different kinds of objects (Fig. 1, left panel). On the basis of this simulation, we set selection criteria. Two bright galaxies M86 (NGC 4406) and M84 (NGC 4374) appear in our field. These two galaxies were surveyed for PNe by JCF, and we can evaluate our selection criteria against the JCF photometry of matched samples. The right panel of Fig. 1 shows the comparison for M84 field, where 74 objects are matched. We found that at least 39% contamination is present in the JCF sample selected by [OIII] line only.

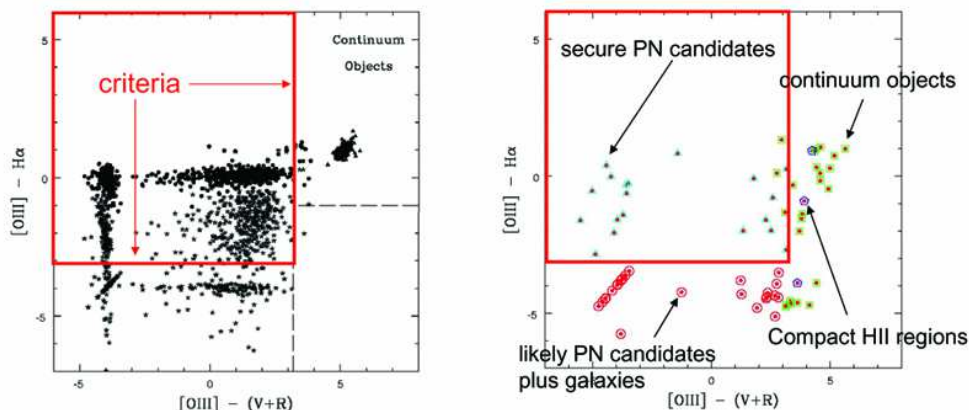


Figure 1. (left) Two-color diagram of the simulated population of point sources. Dots are PNe, stars are single emission-line objects, and triangles are continuum objects. (right) Two-color diagram for the M84 matched sample. Dots are [O III] sources matched to the JCF sample. Triangles (19 objects) indicate the best PN candidates, and circles (26 objects) indicate the single-line emitters, most likely high excitation PNe in this situation. Squares indicate continuum objects. Three pentagons indicate objects with unreliable floating in the intracluster space (Gerhard et al. 2002). Our selection criteria are shown by the thick lines. (Arnaboldi et al. 2003)

### 3.2. Follow-up Spectroscopy for the Virgo Cluster

We carried out follow-up spectroscopy of the ICPN candidates with multifiber FLAMES spectrograph at UT2 on VLT (Arnaboldi et al. 2004). Candidates were drawn from the three survey fields, FCJ, CORE, and SUB, as shown in the left panel of Fig.2. Spectra covered a wavelength range of  $500\text{\AA}$ , centered on  $4797\text{\AA}$  with a resolution of  $\lambda/\Delta\lambda = 7500$ . This gives a velocity resolution of  $40 \text{ km s}^{-1}$  and a typical velocity error of  $12 \text{ km s}^{-1}$ .

A large fraction of the photometric candidates with  $m(5007) < 27.2$  were confirmed and  $\lambda 4959$  line of the [O III] doublet was detected for the first time in about a half of confirmed ICPNe. A total of 40 ICPNe candidates (15/12/13 for FCJ/CORE/SUB fields) were confirmed, and their radial velocities were measured.

Radial velocity distributions of the ICPNe in the three fields are shown in the right panel of Fig. 2. They are considerably different from each other. This confirms the view that Virgo is a highly nonuniform and unrelaxed galaxy cluster, consisting of several subunits that have not yet had time to come to equilibrium in a common gravitational potential.

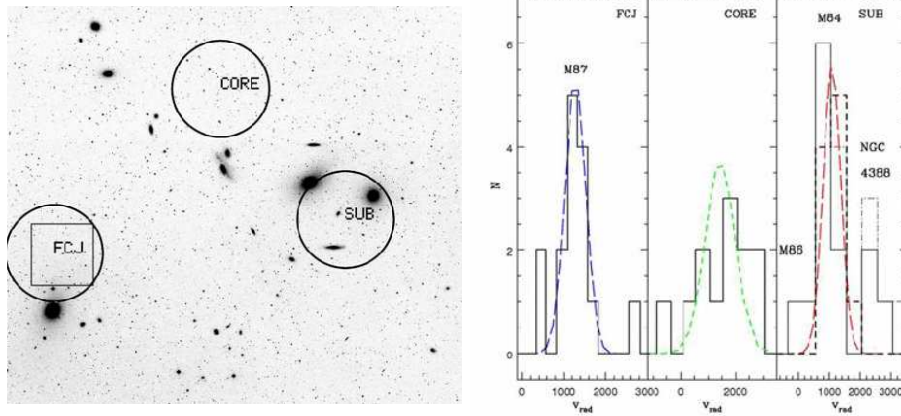


Figure 2. (left) Three fields in the Virgo cluster where follow-up spectroscopy was made. Circles show FLAMES field of view. (right) Radial velocity distributions of ICPNe in the three fields. (Arnaboldi et al. 2004)

## 4. Toward the Coma Cluster

### 4.1. MSIS Technique

As already mentioned, no imaging technique can be successfully applied to the detection of PNe in the Coma cluster. We devised a technique that is similar to the approach used to search for Ly $\alpha$ -emitting galaxies at very high redshift (Stern & Spinrad 1999). It combines multi-slit grism spectroscopy with a narrow band filter centered around the [O III]  $\lambda$ 5007 line at the redshift of the Coma cluster. We use the Faint Object Camera and Spectrograph (FOCAS; Kashikawa et al. 2002) at the Cassegrain focus of Subaru telescope (see Gerhard et al. 2005 for the method and initial results).

A mask of parallel multiple slits is used to obtain spectra of all PNe that happen to lie behind the slits. Because the [O III] emission lines from PNs are only a few kilometers per second wide, their entire flux still falls into a small number of pixels in the two-dimensional spectrum, determined by the slit width and seeing. On the contrary, the sky emission is dispersed in wavelength, allowing a large increase in the signal-to-noise ratio (S/N). The narrow band filter limits the length of the spectra on the CCD detector, so that many slits can be exposed. This technique, which is a blind search, is referred to as the multi-slit imaging spectroscopy (MSIS) technique. No conventional imaging technique can decrease the sky surface brightness in a similar way.

Figure 3 shows the MSIS field and the slit mask. The circular FOCAS field of view (FOV) has 6' in diameter (166 kpc at the assumed distance of 95 Mpc). The spatial resolution of FOCAS is 0.''1 pixel<sup>-1</sup>, so the 6' diameter corresponds to 3600 pixels. The light passing through the narrow band filter and a 0.''6 wide long slit, and dispersed by the grism, projects down to a spectrum of about 43 pixels. A mask was therefore manufactured with uniform long slits spaced every 50 pixels and interrupted only by short sections to ensure mechanical stability.

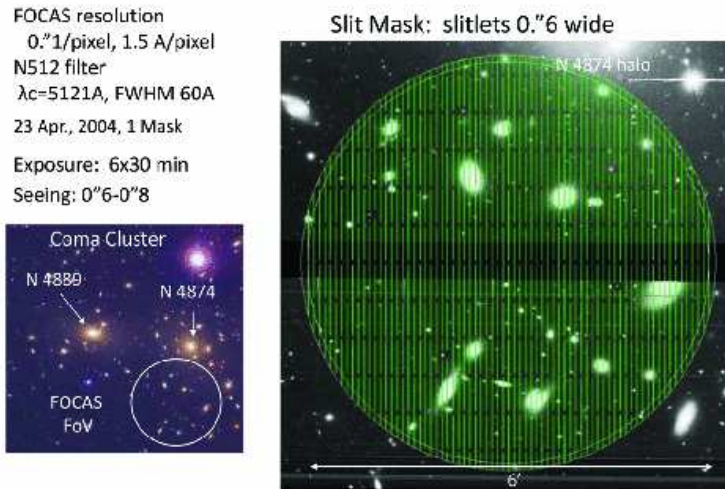


Figure 3. MSIS technique. (left) Location of the MSIS field. (right) Slit mask. (Gerhard et al. 2005)

We used 300B grating, which gives a measured dispersion of  $1.45\text{\AA pixel}^{-1}$  on the two FOCAS CCD chips. The effective spectral resolution is  $7.3\text{\AA}$ , or  $440\text{ km s}^{-1}$ . We also used the N512 filter with FWHM  $60\text{\AA}$ , centered at  $\lambda_c = 5121\text{\AA}$ , the wavelength of the redshifted [O III] emission from a PN at the mean recession velocity of the Coma Cluster ( $6853\text{ km s}^{-1}$ ; Colless & Dunn 1996). The  $60\text{\AA}$  FWHM includes only  $\pm 1.6\sigma$  the velocity dispersion of galaxies. By taking exposures at 8 positions successively shifted along the dispersion direction, we can roughly cover the whole field of view.

#### 4.2. Hint of On-going Subcluster Merger in the Coma Cluster

Observations at three mask positions centered on the field at  $(\alpha, \delta)$  (J2000) =  $(12^h 59^m 41.^s 8, +27^\circ 53' 25.'' 4)$  (see Fig. 3) were carried out during the nights of 2004 April 21-23. We detected a total of 60 emission line objects. Among them, 35 are ICPNe candidates with no continuum flux, 5 are PN candidates projected against the extended halos of Coma member galaxies, and 20 are background galaxies. Details of the data reduction and a catalog of ICPNe candidates are given in Arnaboldi et al. (2007).

Figure 4 shows the velocity histograms of ICPNe (left), Coma galaxies in the MSIS field (middle), and background emission-line galaxies (right). We detect clear velocity substructures of ICPNe, i.e., intracluster stellar population, within a 6 arcmin diameter MSIS field. A substructure is present at  $\sim 5000\text{ km s}^{-1}$ , which is probably from infall of a galaxy group, while the main component is centered around  $\sim 6500\text{ km s}^{-1}$ ,  $\sim 700\text{ km s}^{-1}$  offset from the nearby cD galaxy NGC 4874. The kinematics of ICPNe found in this study and morphology of the diffuse intracluster light (Thuan & Kormendy 1997) show that the cluster core is in a highly dynamically evolving state. In combination with galaxy redshift and X-ray data this argues strongly that the cluster is currently in the midst of

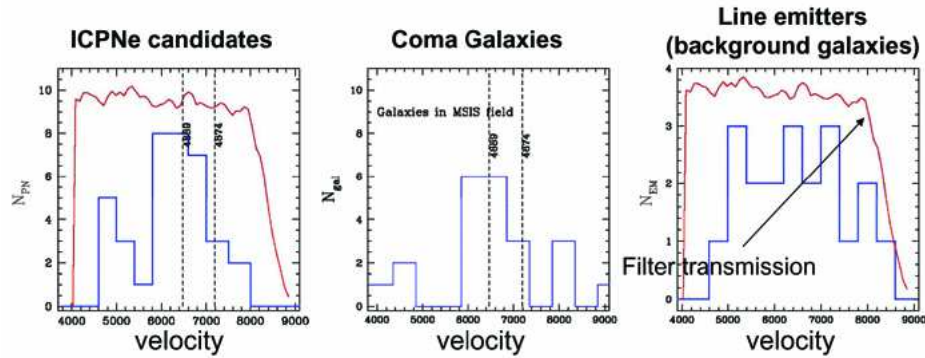


Figure 4. Velocity histograms of ICPNe (left), Coma galaxies in the MSIS field (middle), and background emission-line galaxies (right). Filter transmission curve is shown in the left and right panels. (Gerhard et al. 2007)

a subcluster merger during which the elongated distribution of diffuse light has been created. The two subcluster cores (NGC 4874 and NGC 4889) are presently just after their second close passage. The likely orbits of the subcluster cores are illustrated in Fig. 5. (Gerhard et al. 2007)

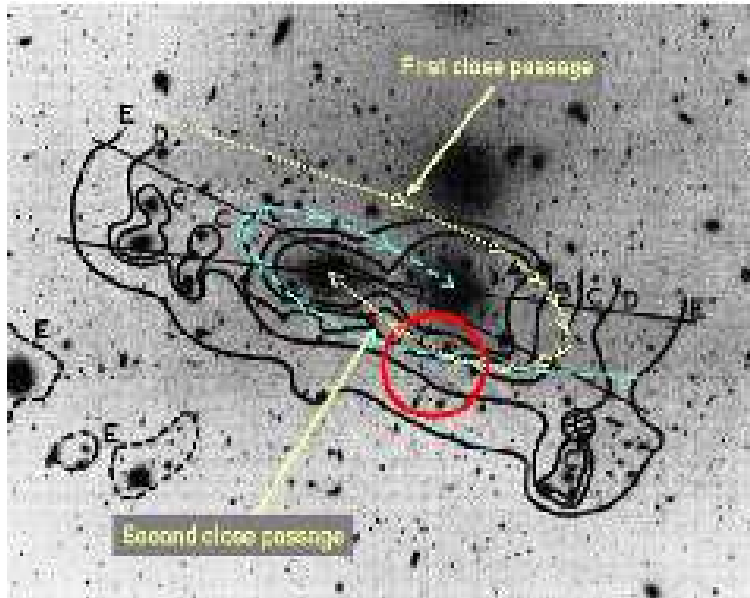


Figure 5. The likely orbits of NGC 4889 and NGC 4874 up to their present positions are sketched. Contours show the surface brightness distribution of diffuse intracluster light taken from Thuan & Kormendy (1997). The circle indicates the MSIS field. (Gerhard et al. 2007)

### 4.3. New Deep Imaging Program for Diffuse Intracluster Light

Inspired by the work by Mihos et al. (2005) and Krick et al. (2006), we started a new very deep imaging program to detect the diffuse intracluster light in a wide  $50' \times 50'$  field centered on the Coma cluster using a CCD camera attached to the 105-cm Schmidt telescope at Kiso observatory, Institute of Astronomy, University of Tokyo. We hope to obtain some data in spring, 2008.

**Acknowledgments.** This work is based on the collaboration with Magda Arnaboldi, Ortwin Gerhard, Ken Freeman, Naoki Yasuda, and Nobunari Kashikawa, and in part with Suprime-Cam team. We thank the staff of Subaru Observatory for their support.

### References

- Arnaboldi, M. et al. 1996, ApJ, 472, 145  
 Arnaboldi, M. et al. 2003, AJ, 125, 514  
 Arnaboldi, M. et al. 2004, ApJ, 614, L33  
 Arnaboldi, M. et al. 2007, PASJ, 59, 419  
 Colless, M. & Dunn, A.W. 1996, ApJ, 458, 435  
 Ferguson, H. et al. 1998, Nat, 391, 461  
 Gerhard, O. et al. 2002, ApJ, 580, L121  
 Gerhard, O. et al. 2005, ApJ, 621, L93  
 Gerhard, O. et al. 2007, A&A, 468, 815  
 Iye et al. 2004, PASJ, 56, 381  
 Jacoby, G. et al. 1990, ApJ, 356, 332  
 Kashikawa et al. 2002, PASJ, 54, 819  
 Krick et al. 2006, AJ, 131, 168  
 Mihos et al. 2005, ApJ, 631, L41  
 Miyazaki, S. et al. 2002, PASJ, 54, 833  
 Okamura, S. et al. 2002, PASJ, 54, 883  
 Stern, D. & Spinrad, H. 1999, PASP, 111, 1475  
 Thuan, T.X. & Kormendy, J. 1977, PASP, 89, 466

### Questions and Answers

*M. Strauss:* How large would the contamination of the Virgo ICPNe sample be by background galaxies if you didn't have the H $\alpha$  filter?

*S.Okamura:* Lower limits of the fraction of contamination estimated from the comparison with FCJ are 39% and 56% for M84 sample and M86 sample, respectively. In a blank intracluster field, the contamination could be much larger. So, the use of H $\alpha$  filter is critically important.

*N. Kawai:* Can you tell whether these ICPNe were originally formed in the member galaxies or formed outside?

*S.Okamura:* Most of them are likely to be formed in the member galaxies and stripped off later during the cluster assembly. It is, however, still an open

question whether or not some ICPNe were formed outside galaxies in the very early phase of cluster formation.

*J. Krick:* G. Bernstein et al. measured the amount of diffuse intracluster light in the Coma cluster to be  $\sim 50\%$  of the total cluster light. How do your values from the ICPNe compare to this?

*S. Okamura:* We have not yet made the estimate for the Coma cluster. It is probably highly unreliable if we make the estimate based on the number of ICPNe detected in the present study over a fraction ( $\sim 3/8$ ) of a single small MSIS field. I hope our new deep imaging program with Kiso Schmidt telescope would give a reliable estimate.

*N. Tamura:* Any estimation of metallicity for ICPNe?

*S. Okamura:* Estimation of metallicity is a very difficult job yet to be done.